Journal of Applied Polymer Science

A Novel Gastric Release PEG-Enclatherated Polymethacrylate-Based Memblet System

Shivaan Cooppan, Yahya E. Choonara, Lisa C. du Toit, Pradeep Kumar, Valence M. K. Ndesendo, Viness Pillay

Department of Pharmacy and Pharmacology, Faculty of Health Sciences, University of the Witwatersrand, Parktown 2193, Johannesburg, South Africa

Correspondence to: V. Pillay (E-mail: viness.pillay@wits.ac.za)

ABSTRACT: A novel polymethacrylate-based membranous system referred to as a *"memblet"* was developed for potential application in controlled gastric drug delivery. A polymethacrylate-based latex, Eudragit® E100, was enclatherated with a 60% w/v and a 30% w/v solution of polyethylene glycol 4000 to form hydrogel formulations A and B, respectively. The hydrogels were subsequently compressed into memblets that were characterized for thermal, rheological, morphological, mechano-chemical properties, and *in vitro* gastric drug release analysis. Molecular mechanics (MM) simulations were performed to corroborate the experimental findings. Critical yield values of 15.39 and 5.239 Pa were obtained for hydrogel A and B, respectively. The viscoelastic region was found to be <10.67 and 2.542 Pa for hydrogels A and B, respectively. The storage modulus was greater than the loss modulus for hydrogel A while the inverse was true for hydrogel B. Thermal, mechanical, and surface morphology evaluation revealed that the converse was true for the dried membrane structure with hydrogel B having superior characterization profiles than hydrogel A. Notably, the lower PEG concentration (30% w/v) displayed better characterization profiles than a higher concentration (60% w/v). Through MM simulations, desirable agreement between the theoretical and experimental results was achieved over the given concentration range of PEG. Based on the gastric drug release analysis, memblets formulated with hydrogel B displayed superior control of drug release. © 2012 Wiley Periodicals, Inc. J. Appl. Polym. Sci. 128: 4327–4338, 2013

KEYWORDS: drug delivery systems; rheology; polymer rheology; calorimetry

Received 16 August 2012; accepted 7 September 2012; published online 25 October 2012
DOI: 10.1002/app.38570

INTRODUCTION

Membranous systems find expression in many modalities of drug delivery.[1–3] A membrane is an interphase between two adjacent phases acting as a selective barrier and modulating the exchange of substances between the two compartments. One of the crucial advantages of membranes includes the transport selectivity of the membrane. Upscaling and downscaling of membrane processes are relatively easy when compared with other methodologies.[4]

Tissue engineering, surface-attachable protein-anchored membranes, organic–inorganic hybrid systems obtained by simultaneous grafting and crosslinking are all well-established applications in membrane technology marking the extensive use of such technologies.[5–7] Hydrogels are porous polymeric networks that retain and entrap large volumes of water within their matrices.[8–10] Selected drug molecules (mostly hydrophilic in nature) can be directly encapsulated within hydrogel networks by triggering self-assembly in the presence of the drug.[11] Polymeric hydrogels exhibit both structural and functional advantages in pharmaceutical research. The authenticity of the hydrogel and the subsequent membrane, with regards to drug delivery, is highly dependent on the reproducibility of drug release, novelty of design, and well-defined physicochemical and physicomechanical properties.[12] Controlled and sustained release from polymeric matrices ensures the delivery of drugs in a predictable manner so as to match physiological needs. However, hydrogels exhibit weak mechanical strength and in certain cases rapid erosion and drug release from the internal matrix.[13]

Membranous systems or scaffolds have been utilized especially for implants due to their ability to retard drug release in a highly site-specific manner. Implant devices formulated through these systems have been known to bypass regular side effects such as inflammation and infection associated with other devices.[14]

Membranous systems derived from hydrogels exhibit weak mechanical properties often producing a very brittle formulation. The use of membranous systems very rarely strays from the implant protocol, due to its high success rate in this field. Many membranous systems have utilized chitosan for its

nontoxic, biocompatible, and biodegradable properties.[15,16] However, this highly abundant polysaccharide does pose limitations particularly with regards to low acidic solubility and an inherent brittleness and stiffness,[17] characteristics that are not suitable for gastric oral drug delivery.

Eudragit polymers (Röhm GmbH and Co. KG, Germany) have been extensively used as coating agents in the modulation of drug delivery.[18,19] Eudragit® E100 is a methacrylic copolymer butyl methacrylate-(2-dimethylaminoethyl)methacrylate-*co*-methyl methacrylate with the monomer ratio of 1 : 2 : 1, respectively. It is a water-soluble polymer consisting of hydrophilic groups, fitting hydrophobic groups and a low viscosity. Eudragit E100 is a preferred polymer over chitosan as it exhibits solubility at pH 1.2–5.0, which is ideal for gastric drug release. [20] Very few studies have been undertaken to utilize Eudragit E100 beyond its conventional use as a coating and taste masking agent.[20,21]

Goddeeris et al.[22] utilized the gastro-protectant property of Eudragit E100 and a surfactant for developing a novel ternary solid dispersion to deliver the poorly soluble UC-781(an anti-HIV drug) in the attempt to enhance its dissolution.[22] This particular study depicts how Eudragit E100 can be utilized beyond its conventional use. Eudragit E100 also displays the potential for use in sustained drug delivery, due to it being minimally impacted on by changes in environmental pH.[23] Specifically, the Eudragit E100 polymer grade requires 30 min to completely dissolve in an acidic environment making the polymer ideal for gastric drug delivery as the gastric transit time can vary between 3 and 4 h. The disadvantage of employing this polymer for drug delivery is that total release occurs within 30 min, which is not a guaranteed controlled release mechanism. The cationic properties of Eudragit E100, which is due to its tertiary amine group, have been useful in the stabilization of other polymers both natural and synthetic. This property has influenced its use as an excipient in pharmaceutical products and in drug-adhesive transdermal systems where it also serves in preventing crystallization of drug.[24]

The purpose of this study, therefore, was to enclatherate Eudragit E100 with a neutral polymer (polyethylene glycol 4000) (PEG) [HO—CH_2— (CH_2—O—CH_2—)$_n$—CH_2—OH] to form a plasticized hydrogel, which when subsequently dried would result in a membranous structure that can be converted to a drug-loaded tablet-like device, we termed a "Memblet" for the gastric release of the model anti-tuberculosis drug rifampicin. Studies conducted on this memblet included surface morphology, mechanical properties, thermal properties, rheological behavior, and *in vitro* drug release studies. In addition, the molecular energy parameters of the aqueous–polymer complex systems at different PEG concentrations were compared using molecular mechanics (MM) simulations by exploring the spatial disposition of Eudragit E100 and PEG with respect to each other and the molecularly interpreted results were corroborated with the rheological data.

MATERIALS AND METHODS

Materials

Eudragit E100 was purchased from Evonik Degussa Africa (Midrand, Gauteng, South Africa), while polyethylene glycol 4000 (PEG 4000) was purchased from Merck Chemicals (Halfway House, Gauteng, South Africa). Acetone, triethyl citrate (TEC), isopropyl alcohol, sodium lauryl sulphate, and Tween 80 were all of analytical grade and used as purchased. Water was purified by a MilliQ Millipore water purification system (Milli-Q, Millipore, Billerica, MA). Rifampicin (RIF) was of analytical grade and obtained from Sigma Aldrich (St. Louise, MO).

Preparation of the Memblet

For manufacture of the memblet system, 34 mL of acetone, 46.9 mL of isopropyl alcohol, and 1.8 mL of deionized water were measured and added to a 200 mL beaker. Affectively, 13.6 g of Eudragit E100 was gradually added to the aforementioned organo–aqueous phase with constant agitation employing a magnetic stirrer at room temperature. This was left under agitation until the Eudragit E100 was completely dissolved. A mixture of TEC, Tween 80, and SLS (1 : 1 : 1) was then gradually added to the latex (q.s. to form 100 mL) and left to stir for 1 h. Simultaneously, 100 mL each of 30% w/v and 60% w/v PEG 4000 aqueous solutions were prepared. A volume of 5 mL of the Eudragit E100 latex was then drawn up and expelled through a syringe into both PEG solutions. Controlled precipitation and PEG enclatheration resulted in hydrogels A (60% w/v PEG 4000) and B (30% w/v PEG 4000) that were subsequently left to cure in their respective solutions for 20 min. Figure 1 depicts the process of the memblet preparation. Following the curing step, the hydrogels were washed thrice in 500 mL deionized water before storage in a desiccant jar (using silica crystals) for 10 days to allow drying. The dried membranes were then ground using a grinder and the powder obtained was evaluated for its powder flow properties and thereafter blended with 150 mg of the model drug rifampicin. The powder blend was then compressed into a tablet like structure termed a *memblet*.

Rheological Analysis of the Plasticized Hydrogels Before Drying

A modular advanced rheometer system (MARS), Thermohaak Rheometer (ThermoHaake, Germany) was employed for the rheological analysis. A cone and plate geometry with a diameter of 35 mm and cone angle of 1° − sensor C35/1°Ti was used for standard rotational studies (yield stress test) and dynamic oscillatory measurements (stress and frequency sweeps in which there was a constant application of sinusoidal shear stress). Samples tested included the Eudragit E100 latex before plasticizing and the plasticized hydrogels before drying using desiccant jars. The hydrogels were used for no more than two tests before a fresh sample was prepared. Separate testing parameters were selected for each sample (latex and hydrogel) as shown in Table I. On reaching full dispersion, the latex was poured directly onto the rheometer plate for analysis. Sample preparation for the hydrogels was more intricate. With regard to rheology, sample preparation is crucial for accuracy, reproducibility, and actual measurement success as hydrogels have the potential to slip from or between the cone and plate during analysis. Methods proposed in previous studies included the use of sand paper glued to the parallel plates with the gap size set at 2 mm to account for the thickness of the sample.[25,26] These methods could be replicated, but proved unsuccessful as the hydrogel was deformed by the sand paper and though slippage was prevented, the required gap size of 0.051 mm was not reached. A successful method was developed by using the cone of the rheometer to compress the sample with ample recovery time between compressions, until the sample was of a uniform surface to reach the required gap size without detrimental deformation. Memblets were prepared

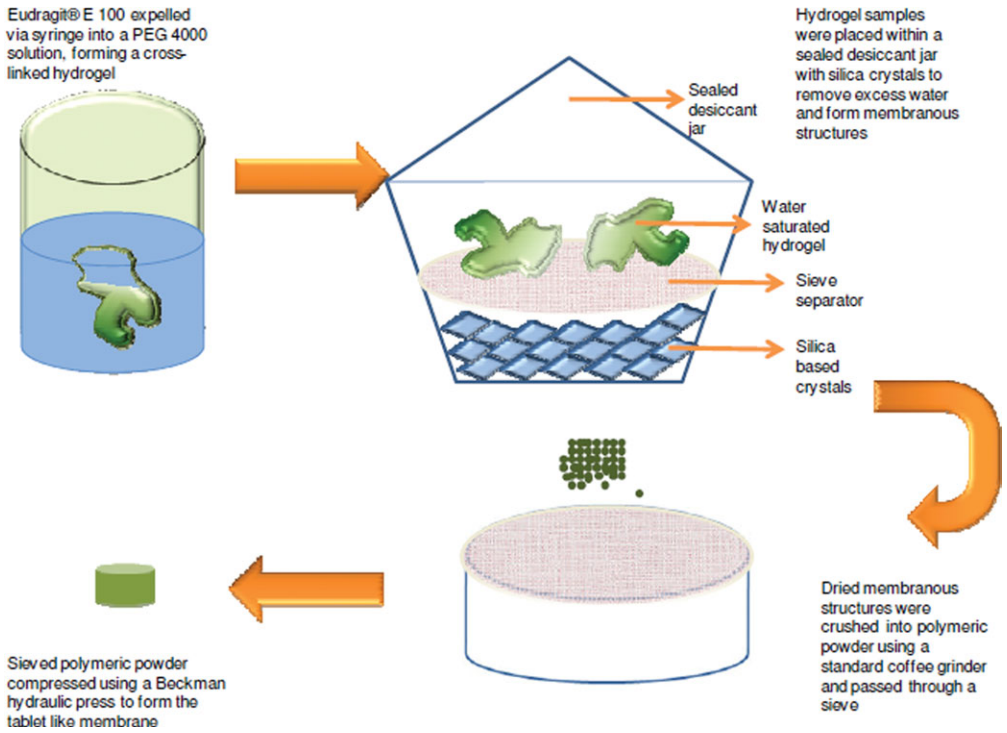

Figure 1. Schematic describing the manufacturing process of the memblet. [Color figure can be viewed in the online issue, which is available at wileyonlinelibrary.com.]

with dimensions that conformed to the gap size of the rheometer. Samples were coated with petroleum jelly to prevent excess water loss during the test.

Thermal Analysis of the Plasticized Polymethacrylate-Based Memblet

Thermal analysis was conducted on a differential scanning calorimeter (DSC) (Mettler Toledo, DSC1, STAR^e System, Swchwerzenback, Switzerland). Testing of memblets was conducted using both basic DSC and alternating DSC (ADSC). All samples were weighed on perforated 40 μL aluminum crucibles. Analysis was conducted using a temperature range of 0–200°C, ramped at 10°C/min under a N_2 atmosphere in order to diminish oxidation. ADSC was performed with an underlying heating rate of 1°C/min and a modulated temperature of 0.1°C per 0.8 min.

Table I. Method parameters for Yield Test, Stress Sweep, and Frequency Sweep Tests

Yield test	E 100 latex	PEG 60%	PEG 60%
Temp (°C)	20	20	20
τ start (Pa)	0	0	0
τ end (Pa)	5	400	400
Duration (s)	200	200	200
Stress sweep		PEG 60%	PEG 30%
Temp (°C)		20	20
τ start (Pa)		0	0
τ end (Pa)		100	100
Frequency (Hz)		0.1–1	0.1–1
Steps		20	20
Frequency sweep		PEG 60%	PEG 30%
Temp (°C)		20	20
Fixed τ (Pa)		6.5	6.5
Start Freq (Hz)		1	1
End Freq (Hz)		0.01	0.01

Assessment of the Surface Morphology of the Memblet

Scanning electron microscopy (SEM) analysis was performed using a Phenom™ SEM (FEI Company, OR). Samples were made electrically conductive before analysis through gold-sputter coating (SPI Module™ Sputter Coater, SPI Supplies, PA) and were attached to an SEM stub using adhesive carbon tape. Argon gas was allowed to flush the system before the leak valve was sealed and the vacuum was turned on. The sputter coater was turned on for 90 s when plasma current reached 18 mA after which the system was turned off and the vacuum released.

Assessment of the Interpolymeric and Intrapolymeric Interactions of the Memblet

Fourier transmission infrared spectroscopy (FTIR) was performed on the individual polymers, Eudragit E100 and PEG 4000 before memblet analysis. A Perkin Elmer Spectrum 2000 FTIR spectrometer with a MIRTGS detector, (PerkinElmer Spectrum 100, Llantrisant, Wales, UK) was used for analysis. Samples were placed on a single bounce diamond crystal and processed by the universal attenuated total reflectance (ATR) polarization accessory for the FTIR spectrum series at a resolution of 4 cm^{-1}. The spectrum was a ratio spectrum of 16 sample scans against 16 ranging from 4000 to 650 cm^{-1}.

Table II. Parameters Employed for Rigidity, Deformation Energy, and Resilience Testing

Parameters	Rigidity	Deformation energy	Resilience
Pretest speed	1 mm s^{-1}	1 mm s^{-1}	1 mm s^{-1}
Test speed	0.5 mm s^{-1}	0.5 mm s^{-1}	0.5 mm s^{-1}
Post-test speed	1 mm s^{-1}	1 mm s^{-1}	1 mm s^{-1}
Compression Force	40 N	40 N	-
Trigger type	Auto	Auto	Auto
Trigger Force	0.05 N	0.05 N	0.05 N
Load cell	5 kg	5 kg	5 kg

Mechanical Evaluation of the Memblet System

Textural profiling was conducted with a Texture Analyzer (TA.XT-*plus*, Stable Microsystems, Surrey, UK) to evaluate memblet deformation energy, flexibility, and resilience. For deformation energy and memblet flexibility, a flat steel probe (2 mm diameter) was used to puncture the memblet matrix. A cylindrical probe, which applied surface pressure to the memblet was used to determine the matrix resilience. Table II shows the parameters selected for each mechanical test.

In Vitro Drug Release Analysis of the Memblet System

Drug release studies were conducted utilizing a USP 33 apparatus II (Erweka DT 700 GmbH Germany) in which a memblet ($N = 3$) was placed within the dissolution vessel under a stainless steel ring-mesh assembly for preventing the paddle inflicting physical/mechanical damage to the memblet and potentially altering the release profiles obtained because of unstable hydrodynamics. Each vessel was contained 900 mL simulated gastric fluid (pH 1.2; 37°C). The rotating paddle method was selected at a rotational speed of 50 rpm and the dissolution apparatus was calibrated for a 2 h run with samples taken at 30 min intervals. Sampling involved the removal of 5 mL of dissolution media with subsequent replenishment of drug-free SGF in order to maintain sink conditions. Samples were then subject to UV spectroscopy analysis for drug concentration analysis.

Static Lattice Atomistic Simulations

All modeling procedures and computations, including energy minimizations in MM, were performed using HyperChem™ 8.0.8 molecular modeling system (Hypercube Inc., Gainesville, FL) and ChemBio3D Ultra 11.0 (CambridgeSoft Corporation, Cambridge, UK). The octamers of Eudragit E100 and PEG were drawn using ChemBio3D Ultra in its syndiotactic stereochemistry. The models were initially energy-minimized using the MM+ force field (ChemBio3D Ultra 11.0) and the resulting structures were again energy-minimized using the AMBER 3 (assisted model building and energy refinements) force field (HyperChem 8.0.8). The conformer having the lowest energy was used to create the polymer–polymer complexes. Full geometrical optimization was performed in vacuum employing the Polak–Ribiere conjugate gradient algorithm until an RMS gradient of 0.001 kcal mol^{-1} was reached. Force field options in the AMBER (with all H-atoms explicitly included) and MM+ (extended to incorporate nonbonded cutoffs, restraints, and periodic boundary conditions) methods were set as defaults. For MM computations, the force fields were utilized with a distance-dependent dielectric constant scaled by a factor of 1. The 1–4 scale factors were electrostatic 0.5 and van der Waals 0.5. To generate the final models in solvated system the MM simulations were performed for cubic periodic boxes with the polymer–polymer complex at the center of the cubic box and the remaining free-space filled with water and the same procedure of energy-minimization was repeated for generating the solvated models except that the force fields were utilized with a distance-independent dielectric constant with no scaling. Additionally, the force field options in the AMBER (with explicit solvent) were extended to incorporate cutoffs to inner and outer options with the nearest-image periodic boundary conditions, and the outer and inner cutoffs were to ensure that there were no discontinuities in the potential surface.

RESULTS AND DISCUSSION

Evaluation of Memblet Preparation

Eudragit E100 is a water-insoluble and aqueous acid-soluble polymethacrylate polymer with high solubility in water-miscible organic solvents such as ethyl alcohol, isopropyl alcohol, and acetone. PEG 4000 is an amphiphilic polymer soluble in both aqueous and organic phases. In this study, we propose that when Eudragit E100 (dissolved in water-miscible organic solvents) was immersed in an aqueous media gradual precipitation occurred and provided sufficient time for the amphiphilic PEG 4000 to move in between adjacent Eudragit E100 chains. This produced a PEG 4000-enclatherated-Eudragit E100 network that evolved into a membranous structure because of "fusogenesis" of PEG 4000 and the "film-forming" ability of Eudragit E100.

Rheological Analysis of the Plasticized Hydrogels Before Memblet Formation

Determination of Critical Yield Point for the Polymethacrylate-Based Latex and Novel Plasticized Complex Hydrogels. Rheological evaluation was conducted on the Eudragit E100 latex before plasticizing to assess whether the latex was produced in an accurate and reproducible manner. This is due to the fact that during preformulation studies, an inconsistently formulated hydrogel matrix led to the formation of an erratic membrane that was nonreproducible. Latex solutions of 10 mL were plasticized and cured in their respective plasticizing PEG solutions producing 30% w/v and 60% w/v hydrogels. The yield stress values for all samples are shown in Figures 2(a–c). Typically, Eudragit E100 latex samples before plasticizing showed similar critical yield points [Figure 2(c)]. Yield stress tests resulted in an average critical yield point of 0.36 Pa that correlated to the viscous nature of the latex. The consistent yield point can be attributed to the astringent and meticulous method used for preparing the latex each time. It could be postulated that there were no major and highly altering physicochemical interactions and that the distribution of the particles was isotropic. No mechanical alteration or damage to the latex was incurred. All samples had close deformation (γ) points at the 57.73 s^{-1} region, indicating that this was the region at which the latex behaved in a fluid-like manner.

For analysis of the hydrogels, the critical yield point was determined to assess maximal plasticizing potential of the novel membranous system subsequent to the drying protocol. Critical yield points were dependent on formulation parameters such as

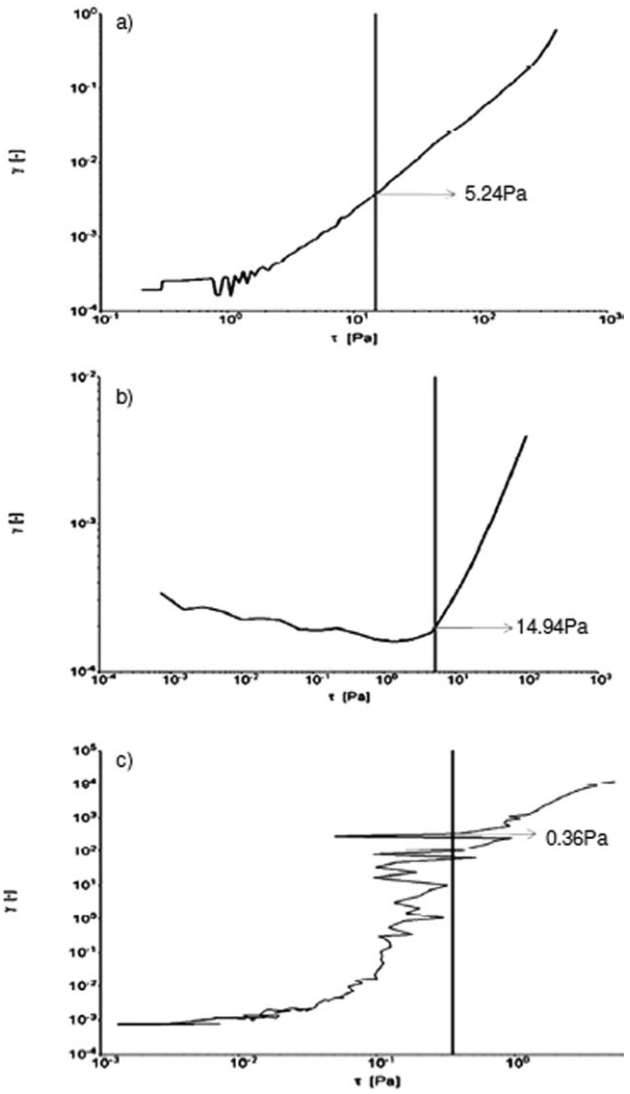

Figure 2. Yield stress curves for (a) formulation A, (b) formulation B and (c) the latex before plasticizing to indicate the critical yield point (Pa).

the type of plasticizer, plasticizer concentration, and temperature. For the purposes of this study, the type of plasticizer (PEG 4000) and temperature (20°C) were kept constant, such that emphasis was placed on determining the effect of plasticizer concentration on hydrogel deformation. Yield stress curves for hydrogels A and B indicated membrane flexibility for both formulations but variance was noted in that hydrogel A achieved a greater critical yield point (14.94 Pa) compared with hydrogel B (5.23 Pa) (Figure 2). This can be explained with an understanding of the properties of hydrogels. Hydrogels are defined as three-dimensional hydrophilic polymer networks, which when in their swollen state, have the capability to retain water and swell to a much larger size than their original state.[27,28] Physical ionic plasticizing occurred between the ether functional group (anionic) of PEG 4000 and the dimethyl aminoethyl methacrylate functional group (cationic) of Eudragit E100 resulting in an interpolyelectrolyte complex hydrogel. Hydrogel A consisted of a higher degree of saturation of functional groups, with regard to plasticizing, that resulted in a dense accumulation of PEG 4000 to produce a more rigid structure. In addition, the presence of fewer free functional groups along the polymeric backbone of hydrogel A (as compared to hydrogel B) because of the higher degree of plasticizing in 60% w/v PEG 4000 solution impeding the polymeric backbone's mobility. This dense accumulation of polymeric material rendered hydrogel A less flexible rheologically. Both factors resulted in retarded molecular mobility. Molecular movements, owing to the fewer free functional groups was improved in hydrogel B, indicating a more flexible and versatile formulation.

Viscoelastic Evaluation Through Stress Sweep Curves of the Novel Plasticized Complex Hydrogels. The viscoelastic region for each hydrogel was determined such that a value for input into the frequency sweep curves to generate values of G′ (storage modulus) and G″ (loss modulus) could be obtained. The stress sweep curves suggested nonlinear complex viscoelasticity (shear thickening) as an increase in G′ was observed with an increase in oscillating stress.[29,30] The nonlinear viscoelastic regions for the hydrogels are shown in Figure 3. The presence of a viscoelastic region in both samples confirmed that the hydrogels were viscoelastic materials displaying both solid and liquid properties. Hydrogel A demonstrated a viscoelastic region below 10.67 Pa and hydrogel B was below 2.542 Pa corroborating the findings in yield stress that flexibility was improved in hydrogel B.

Determination of the Storage (G′) and Loss (G″) Modulus of the Novel Plasticized Complex Hydrogels. The semisolid hydrogels were evaluated and found to encompass viscoelastic properties through the stress sweep curves. As such the hydrogels displayed both elastic (solid) and viscous (liquid) properties, which could be determined simultaneously through frequency sweep tests. Oscillation stress sweep was used to obtain the viscoelastic region. The viscoelastic region was frequency dependent and therefore stress sweep was performed over three frequencies (0.01, 0.1, and 1 Hz). The strength and subsequently the stability of the system correlates with its yield value. As the elastic modulus decreased, the system underwent structural deformation. The stress at which the system exhibited nonlinear behavior was considered the yield stress (τ). In testing both hydrogel samples, frequency ranges of 1–0.01 Hz and a τ value of 6.5 Pa were selected to assess the effect on loss and storage moduli at the same parameters. For a frequency sweep

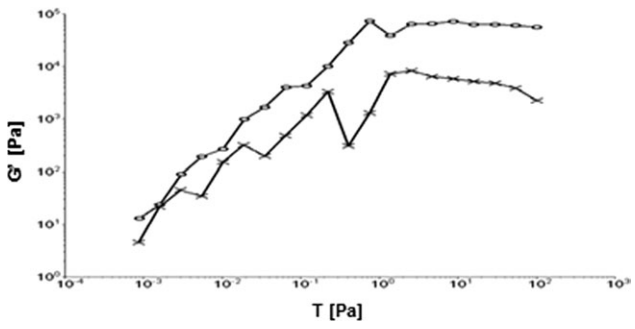

Figure 3. Viscoelastic regions of hydrogel A (O) and hydrogel B (X).

Applied Polymer SCIENCE

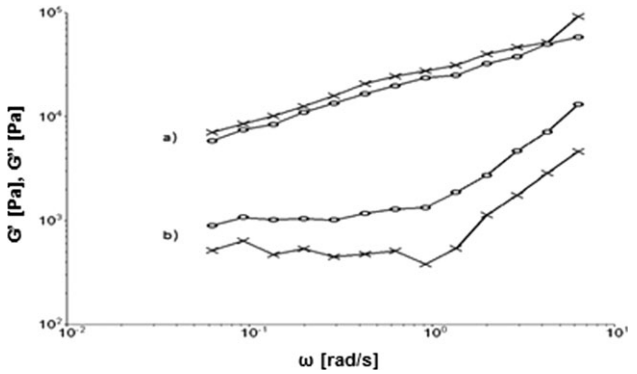

Figure 4. Dynamic oscillation curves depicting storage (G′-X) and loss (G″-O) moduli of: (a) hydrogel A and (b) hydrogel B.

test, G′ was used as a measure of the deformation energy stored within the sample during the shearing process. G′ was therefore a measure of the elastic (solid) nature of the sample. The G″ was a measure of deformation energy used in the sample during the shearing process and lost to the sample afterward, making G″ a measure of the viscous (liquid) nature of the sample.[31] Figure 4(a, b) depicts very different rheological responses for hydrogels A and B with the same testing parameters. Hydrogel A had a continuous curve in which the constant G″ was indicative of a solid, immobile, and elastic structure for all of the frequency ranges and with no G′/G″ crossover. Within the test parameters, the formulation remained elastic for all shear rates and shear forces. The accumulation and saturation of PEG 4000 resulted in an elastic membrane, which would require larger shear forces to achieve the desired mobility. Hydrogel B however can be described as having gel-like properties.[32] At the same testing parameters, Hydrogel B displayed the converse of hydrogel A with G″ > G′ for all frequency ranges indicating highly mobile characteristics. Such a curve was obtained because of lower plasticizing in Hydrogel B compared to Hydrogel A. The formation of bonds between functional groups of both Eudragit E100 and PEG 4000 were evenly distributed within Hydrogel B because of a lower plasticizer concentration. This enhanced flexibility and improved rheological properties promoted the use of a lower concentration of plasticizer in comparison to high plasticizer content.

Assessment of the Interpolymeric and Intrapolymeric Interactions of the Memblet. This assessment was conducted to evaluate any unforeseen chemical interactions between molecules, surface morphologies, and the extent of plasticizing that occurred between the hydrogel samples. FTIR analysis of the Eudragit E100 and PEG 4000 was conducted separately to determine the functional groups of these grades of polymers. Figure 5(a) shows the characteristic bands of the ester groups at 1150–1190 cm^{-1}, 1240 cm^{-1}, and 1270 cm^{-1}, as well as the C=O ester vibration at 1730 cm^{-1}. In addition, CH_X vibrations were discerned at 1385 cm^{-1}, 1450–1490 cm^{-1}, and 2950 cm^{-1}. The absorptions at 2770 cm^{-1} and 2820 cm^{-1} were assigned to the dimethylamino groups of Eudragit E100.[33] The wide and intense band at 3300–3500 cm^{-1} was assigned to the presence of O—H groups and the stretching bands at 2700–3000 cm^{-1} represented the C—H alkyl stretching vibrations of PEG 4000.[34]

These two functional groups allowed for plasticizing that occurred between the two polymers that resulted in the membranous structure. When comparing hydrogels A and B [Figure 5(b)], it was evident that hydrogel B displayed sharper and more defined peaks compared with hydrogel A. Peak sharpness was observed when FTIR was performed on the native powdered polymers and then compared to the compressed form. The bonding between the primary alcohol and the amine group in hydrogel B was evidently more prominent compared to hydrogel A that may have contributed to the greater membrane flexibility. This also implied that a 30% w/v of PEG 4000 may be the upper limit of plasticizing for saturation of bonding between functional groups and that any higher concentrations may lead to weaker flexibility and compromised rheological properties.

Assessment of the Surface Morphology of the Memblet. SEM of the different memblet formulations substantiated the results obtained in FTIR analysis, which indicated that memblet B had superior mechanical properties than memblet A. SEM images of formulation B [Figure 6(b)] revealed a consistently even surface without many crevices, cracks, or large pores. A scattering of white, powder-like debris could be seen and this was attributed to the sodium lauryl sulphate that may have been in excess. The uniformity of structure and surface morphology gives an indication of the solid structural integrity of

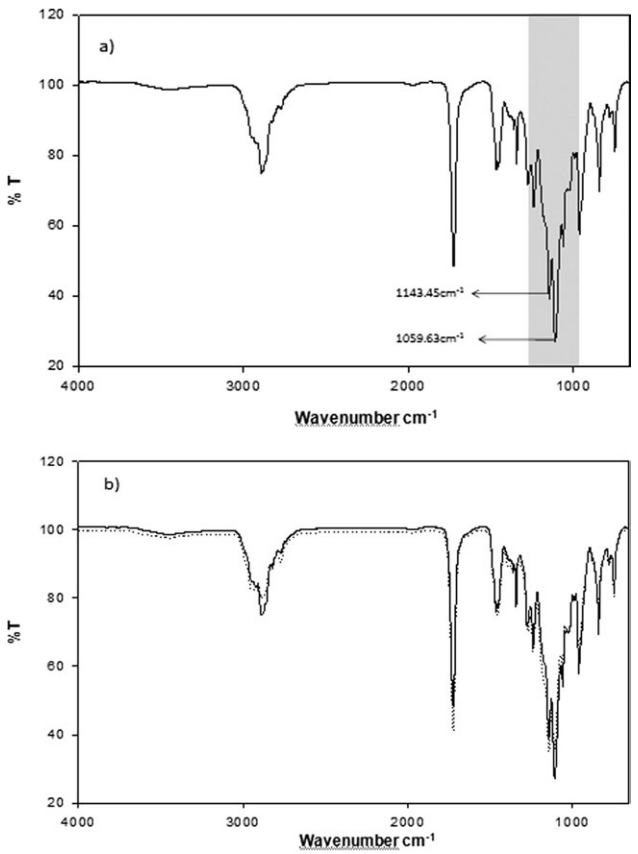

Figure 5. FTIR analysis representing (a) bonding of functional groups between PEG 4000 and Eudragit® E100 and (b) formulations A and B overlaid (A: solid line and B: dotted line).

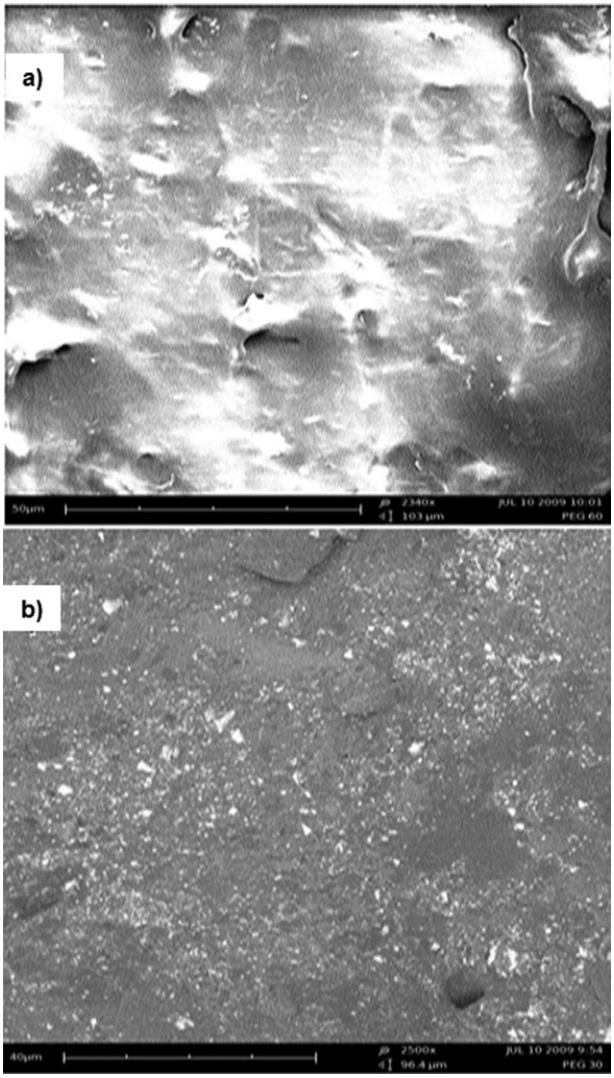

Figure 6. Scanning electron micrographs of (a) formulation A and (b) formulation B.

the formulation. As for memblet formulation A, a notable difference in surface morphology was seen [Figure 6(a)]. A greater quantity of surface debris was present compared to formulation B. This was attributed to a buildup of polymeric material of nonplasticized PEG 4000 and sodium lauryl sulphate, which were viewed as congested white areas. This may have had a detrimental effect on thermal and mechanical properties because of the amount of nonplasticized polymer segments. Memblet formulation B had a large number of fissures and pores relative to formulation A and this further influenced the structural integrity. Uniformity was not seen clearly throughout the imaging. Certain areas had a surface structure similar to memblet formulation B, whereas other areas showed a buildup of polymeric material. It was postulated that in areas with buildup, surface concentration of PEG 4000 on drying had occurred because of leaching of PEG 4000. The dumping prevented optimal saturated plasticizing to occur leaving a weaker interpolymeric structure. This was further investigated through textural and thermal analysis.

Thermal Analysis of the Plasticized Polymethacrylate-Based Memblets

Thermal characterization was conducted in triplicate to identify any abnormalities or detrimental changes to the sample after the plasticizing process and to identify the thermal stability of the drug delivery system. The plasticizing of both memblet formulations A and B with PEG 4000 and the incorporation of TEC allowed for a synergistic plasticizing effect. This was of significant importance as plasticizers, whilst causing a reduction in polymer–polymer chain entanglement, secondary bonding with polymer chains, a reduction in the glass transition temperatures (T_g), increased flexibility and elongation at break and a decreased Young's modulus.[35,36] Plasticizers increased the free volume between polymer chains and in this case, the polymer chains of Eudragit E100. The absence of plasticizer would have led to a highly solid but brittle product unsuitable for oral drug delivery. PEG 4000 comprises polar hydroxyl functional groups and it was the H-bonds formed from these hydroxyl groups that replaced the polymer–polymer bonds within the Eudragit E100 chains, thus producing the plasticizing effect.[36] Additionally, PEG 4000 served as a plasticizing agent for the Eudragit E100 and allowed for the increase in resistance to acidic gastric degradation (through hydrolytic cleavage) of Eudragit E100. Owing to the considerable length of PEG 4000, plasticizes creating a void between the Eudragit E100 chains, the network formed has enhanced free volume leading to the plasticizing effect. TEC served as a stabilizer due to its low volatility and its high miscibility with Eudragit E100.

Memblet formulations A and B were tested under the same formulation parameters during thermal analysis. DSC results were very similar for both formulations and a drastic decrease in glass transitions was observed for both formulations [Figure 7(a, b)]. DSC was run twice utilizing the same temperature programs. The second run was selected for analytical purposes (since thermal information deemed to be more accurate in a second run due to the removal of any thermal history). Memblet formulation A displayed a reduced relaxation peak compared with formulation B [Figure 7(a, b)]. This was defined by the lower integral value of −14.01 mJ for formulation A compared to the −137.95 mJ for formulation B. This implied that more energy was required from the heating system (for formulation B) to allow for a first-order energy transition (melting) to occur. Overall, the thermograms revealed curves that were not the definite peaks, melting points, or the gradual curve of a glass transition but rather hybridization (Figure 7). As PEG 4000 and Eudragit E100 have very similar melting and glass transition temperatures (both between 40−60°C), ADSC was used to separate the curves overlapping thermal events. A more intricate look into the thermal characteristics of the hydrogels was obtained through the C_p-Complex, reversible, and total heat flow curves. The heat capacity from the DSC curve was computed by dividing the heat supplied by the resulting temperature increase or changes in temperature and provided us with an indication of the quantity of energy or heat that was required to increase the sample temperature by a specified amount. Heat capacity can best be described by eq. (1), that is, heat flow (HF) divided by the heating rate (HR). Complex heat

Applied Polymer SCIENCE

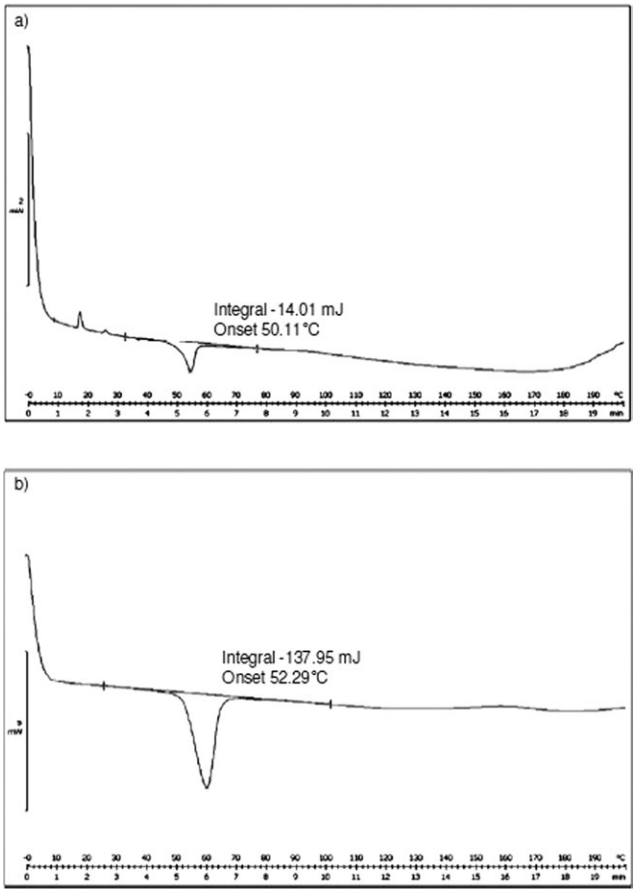

Figure 7. DSC thermograms of (a) formulation A and (b) formulation B.

capacity of the ADSC curve can be defined as the amplitude of the heat flow (AHF) modulation divided by the amplitude of the heating rate modulation (AHR) as shown in eq. (2).

$$C_p = \frac{HF}{HR} \quad (1)$$

$$C_p\text{complex} = \frac{AHF}{AHR} \quad (2)$$

Where HF = heat flow, HR = heating rate; AHF = amplitude of the heat flow and AHR = amplitude of the heating rate modulation.

As shown in Figure 8, the glass transition and the melting point have been separated and shown on the reversible heat-flow and total heat-flow curves, respectively. The melting point remained the same for both formulations at 59°C and only a slight variance was noted in the glass transition. As previously described, PEG 4000 and TEC have a compounded effect of lowering the glass transition point. Memblet formulation A with a higher PEG 4000 concentration (60% w/v) compared to formulation B (30% w/v), displayed a slightly lowered glass transition of 55°C and 56°C, respectively. The C_p-complex (Figure 9), however, showed that formulation A utilized marginally less energy (endothermically) than formulation B for the melting point to be reached. This provided us with an indication that formulation B possessed a slight improvement in mobility. The optimal plasticizing concentration could therefore be expressed as being around the 30% w/v region, corroborating the rheological studies. In general, it can be noted that the formulation methodology produced formulations that have acceptable thermal stability for all concentrations of plasticizer, with a minor improvement noted in the lowered plasticizer concentration (i.e., 30% w/v). Coupled with FTIR analysis and textural analysis, this further highlighted the concept that 30% w/v PEG 4000 was optimal and also provided a better indication to the relative strength of the bonds involved.

Mechanical Evaluation of the Memblet

Mechanical evaluation of memblets was performed on each formulation in triplicate. For both formulations, typical force–distance profiles were generated to evaluate both the deformation energy and flexibility of the formulations [Figure 9(a, b)]. In the textural analysis profile, the gradient represented the memblet flexibility, whereas the area under the curve (AUC) revealed the deformation energy for each sample. The results displayed in Table III are convincing that memblet formulation B had superior mechanical properties. Almost identical values were obtained for both membranes in terms of resilience and deformation energy (Table III). As described earlier, this was attributed to the high plasticizing concentration in both systems allowing for saturated ionic bonds to be formed. The memblet flexibility results were however different. Memblet formulation B, with a lower plasticizer concentration, displayed greater membrane flexibility (7.173 N mm for formulation B vs. 6.293 N mm for formulation A, Table III). This clearly indicated that

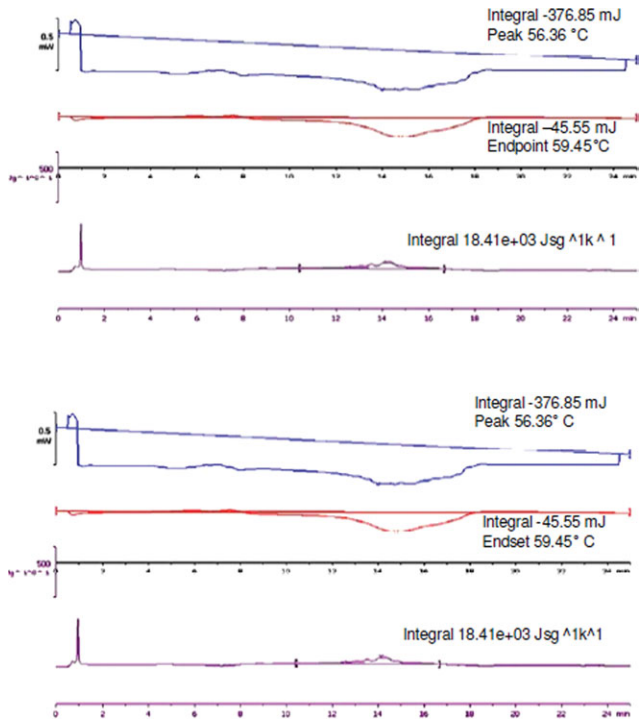

Figure 8. ADSC thermal profiles of (a) formulation A and (b) formulation B. [Color figure can be viewed in the online issue, which is available at wileyonlinelibrary.com.]

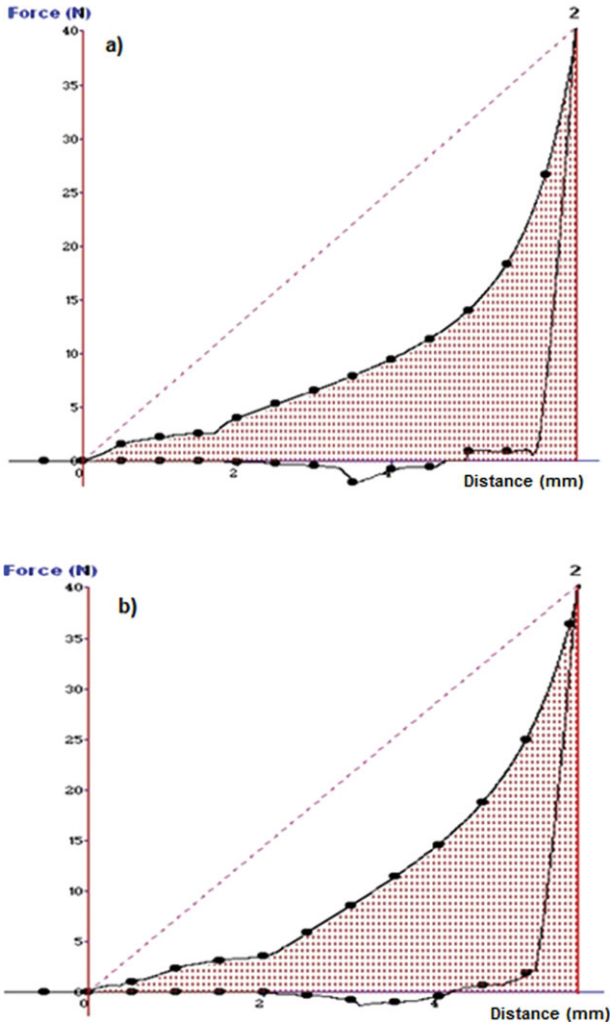

Figure 9. Force-distance profiles depicting matrix resilience, memblet flexibility, and deformation energy for (a) formulation A and (b) formulations B. [Color figure can be viewed in the online issue, which is available at wileyonlinelibrary.com.]

formulation B had superior flexibility, whereas formulation A retained a more rigid nature. Furthermore, this analysis indicated that there was a maximal plasticizer concentration around the 30% w/v region. Much higher concentrations (e.g., 60% w/v) did not result in any significant improvement in the mechanical properties of the memblet.

In Vitro Drug Release from the Memblet

Drug release characteristics for the memblet were targeted to be highly specific for the gastric environment. *In vitro* testing aimed to achieve as close to zero-order release of the model drug rifampicin as possible within a 2 h threshold. Complete release of rifampicin needed to be accomplished such that the majority of rifampicin would achieve gastric absorption and a fractional quantity would be concurrently released in the small intestine. At 0.5 h, both formulations display a general burst effect. The memblet restricted the release to 40% of total drug in comparison to 70% in the control sample. It was postulated that the limited rheological properties of the viscoelastic memblet, provided the slight burst effect as the SGF and mechanical rotation of the spindle (to mimic gastric churning) accelerated the conversion of the memblet to more viscous state compounding erosion. Despite this, burst release of drug was still limited in comparison to the control formulation. From 0.5 to 2 h, a far more controlled drug release pattern was observed. Retardation of drug release was attributed to the improved thermal, mechanical, and intermolecular characteristics of the memblet. The improved molecular bonding through a lowered plasticizer concentration (30% w/v PEG 4000) enforced more rigid intermolecular bonding. Enhanced structural integrity, thermal rigidity, and intermolecular attraction has been achieved and detailed in mechanical, thermal, and FTIR analysis. The thermal strength allowed the memblet to erode at a slower rate as per the elevated glass transition temperature that required greater energy to undergo a phase transition and begin erosion thus controlling drug release. This regulated release pattern was compounded by the improved intermolecular bonding indicated through FTIR and textural analysis. Furthermore, the maximal plasticizing concentration of 30% w/v PEG 4000 did not induce dumping of sodium lauryl sulphate as debris, in comparison to the control formulation as confirmed by the SEM images obtained and described earlier. The compounded effect was to produce a robust gastric delivery system with a controlled drug release pattern. The drug release dynamics can be described as deliberately controlled from 0.5 to 2 h through erosion of the memblet (Figure 10).

Table III. Textural Analysis Results for the Memblet System

Formulation	Resilience (%)	Flexibility (N mm)	Deformation Energy (J)
A	17.6	6.293	0.062
B	17.6	7.173	0.060

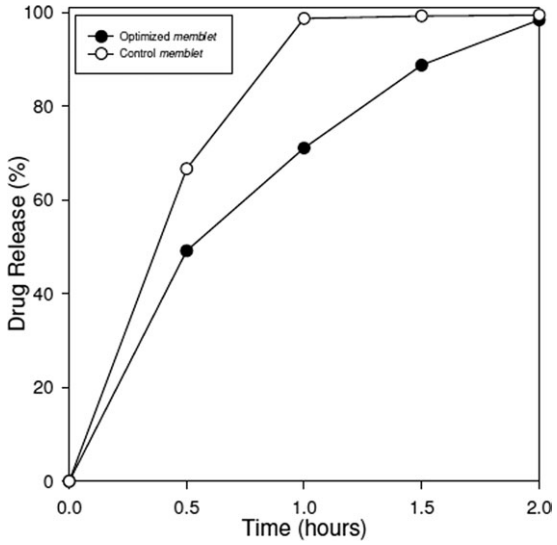

Figure 10. Comparative drug release profiles of the memblet and a control formulation in simulated gastric fluid ($N = 3$; SD < 0.222 in all cases).

Applied Polymer SCIENCE

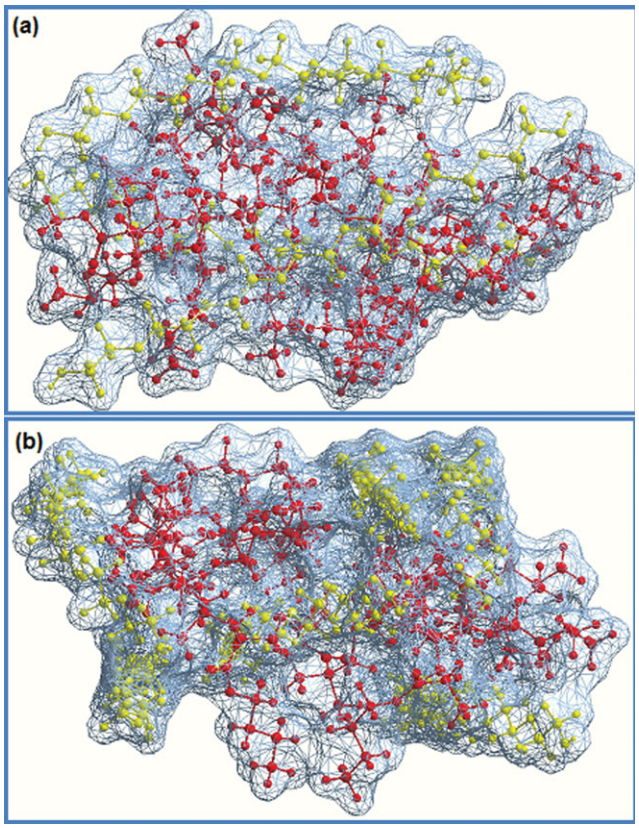

Figure 11. Connolly molecular electrostatic potential surfaces in wire-mesh display mode showing the polymer–polymer complexes in vacuum: (a) EUD_2-PEG_3 and (b) EUD_2-PEG_6; color codes for polymers—Eudragit E100 (red) and PEG 4000 filaments (yellow). [Color figure can be viewed in the online issue, which is available at wileyonlinelibrary.com.]

Computational Analysis and Energetic Expression of the Viscoelastic Properties of the Eudragit E100-PEG 4000 Hydrogel Network

The measured viscoelastic rheological properties may depend on confounded geometry and the extent of network innervations. This requires geometrically proportional networks for all simulations to systematically control and isolate the effects of a given parameter. In this study, we thus used the two representative networks shown in Figures 11, 12, and 13 for computations and randomly removed PEG 4000 from the networks to allow water molecules within the solvent system. PEG 4000 filaments longer than the width of the simulation domain were severed to reduce finite size effects. Therefore, for undertaking the static lattice atomistic simulations for the polymer–polymer complexes in vacuum, one polymer molecule with another was assembled by disposing the molecules in a parallel way to generate the final models: EUD_2-PEG_3 and EUD_2-PEG_6 represented hydrogel B, hydrogel A and an interaction of PEG 4000 with Eudragit E100, respectively. For solvated systems, EUD_1-PEG_2 and EUD_1-PEG_4 represented hydrogel B and hydrogel A, respectively.

It was evident from Table IV that the formation of EUD_2-PEG_3 and EUD_2-PEG_6 (in vacuum) was accompanied by energy stabilization of -55.045 kcal mol^{-1} and -90.788 kcal mol^{-1}, respectively. This confirmed the compatibility of the polymers and

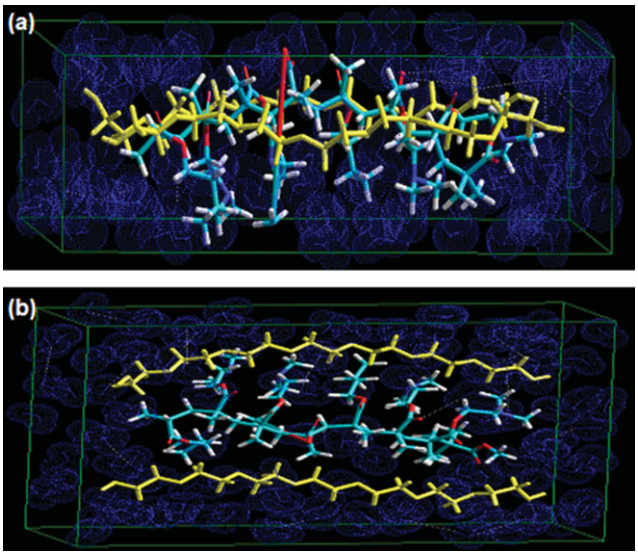

Figure 12. Visualization of geometrical preferences of Eudragit E100 (standard element color) in the presence of PEG 4000 filaments (yellow): EUD_1–PEG_2 (a) lateral view and (b) upper view after molecular simulation in a solvated system consisting water molecules (blue); color codes: C (cyan), N (blue), O (red), and H (white). [Color figure can be viewed in the online issue, which is available at wileyonlinelibrary.com.]

stability of the hydrogel in the dried state. Furthermore, the energy data displayed the involvement of nonbonding interactions in the form of van der Waals forces. These underlying chemical interactions may have induced conformational changes that were responsible for mechanical strength and viscoelastic characteristics of the hydrogels. The weak van der Waals forces also caused aggregation of the aliphatic chains with localized

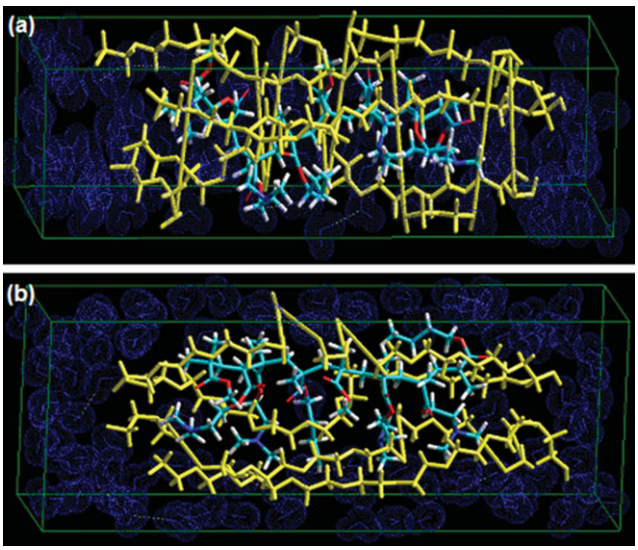

Figure 13. Visualization of geometrical preferences of Eudragit E100 (standard element color) in the presence of PEG 4000 filaments (yellow): EUD_1-PEG_4 (a) lateral view and (b) upper view after molecular simulation in a solvated system consisting water molecules (blue); color codes: C (cyan), N (blue), O (red), and H (white). [Color figure can be viewed in the online issue, which is available at wileyonlinelibrary.com.]

Table IV. Calculated Energy Parameters (kcal mol^{-1}) of the Polymer–Polymer Assemblies Consisting of Eudragit E100 and PEG After Molecular Mechanics Simulations in Vacuum and Solvated Systems

	Energy (kcal mol^{-1})							
Structure	Total[a]	ΔE[b]	Bond[c]	Angle[d]	Dihedral[e]	VDW[f]	H bond[g]	Elec[h]
E 100	77.481	-	8.291	44.796	11.934	12.459	0	0
PEG	11.822	-	0.187	0.844	7.002	3.790	−0.016	0
EUD_2-PEG_3	135.383	−55.045	17.051	85.400	53.559	−20.628	0	0
EUD_2-PEG_6	136.106	−90.788	19.094	82.488	74.214	−39.691	0	0
E100 solvated	−2975.317	-	54.971	110.674	43.466	566.614	−4.142	−3746.9
PEG solvated	−2074.798	-	26.521	31.717	34.332	148.965	−5.591	−2310.74
EUD_1-PEG_2	−1806.173	3243.94	37.276	84.681	67.843	299.288	−5.511	−2289.75
EUD_1-PEG_4	−866.995	4183.12	46.345	260.545	79.455	485.053	0	−1738.39

[a]Total steric energy for an optimized structure, [b]$\Delta E_{interaction}$ = E(Host: Guest)− E (Host) − E(Guest), [c]Bond stretching contributions, reference values were assigned to all of a structure's bond lengths, [d]Bond angle contributions, reference values were assigned to all of a structure's bond angles, [e]Torsional contribution arising from deviations from optimum dihedral angles, [f]van der Waals interactions due to nonbonded interatomic distances, [g]Hydrogen-bond energy function, [h]Electrostatic energy.

regions having a density and refractive index that was different from that of the bulk polymers (Figure 11). Figure 11(b) displays the comparatively dense architecture in case of EUD_2-PEG_6 compared with EUD_2-PEG_3 in Figure 11(a). Additionally, the absence of double bonds, aromatic system, and a sterically hindered environment in this multimolecular assembly may have further increased the tendency of agglomeration as evidenced from the dense architecture in the case of EUD_2-PEG_6 compared with EUD_2-PEG_3.

Surprisingly, the MM simulations for the solvated systems depicted an opposite trend. Both systems, EUD_1-PEG_2 and EUD_1-PEG_4, displayed an increase in binding energy by 3243.94 kcal mol^{-1} and 4183.12 kcal mol^{-1} (Table IV). Additionally, the EUD_1-PEG_4 (hydrogel A) was more destabilized compared with EUD_1-PEG_2 (hydrogel B). This energy difference was mainly due to the electrostatic energy function in both polymer complexes (Table IV). This was attributed to the intrachain repulsion in the ionized polymeric-complex model, where all carboxylic and other functional groups, when fully charged, contributed unfavorably to the electrostatic potential energy and the flexibility of the chain segment decreased (Figure 13). The PEG 4000 region, being hydrophilic, created a highly charged zone, which concentrated a great number of water molecules and hence favored solvation of monomers nearby PEG 4000 (EUD_1-PEG_2) (Figure 12). However, an extensive increase in PEG 4000 filaments may have also resulted in less solvated architecture by the steric hindrance produced at their region. Furthermore, the effect produced by PEG 4000 decreased with distance and this in turn caused an increase in energy (EUD_1-PEG_4) (Figure 13). This increase in steric energy accompanied by a lower solvation increased the yield stress of hydrogel A, thereby corroborating the experimental studies shown in Figure 2.

All mechanical properties were expressed in terms of energy where elasticity (G′) reflected the mechanical energy of deformation stored in a polymer, and viscosity (G″) was a measure of the energy dissipated per molecular passing event. Nevertheless, we found features that semiquantitatively captured experimentally observed behaviors of Eudragit E100 networks in the presence of PEG 4000 filaments. The periodic box dimensions were kept constant in order to apply a prestrain on the polymeric network (Figures 12 and 13). Once the periodic box dimensions were constant, the expansion of the polymeric network during energy minimization experienced a prestrain proportional to the bulk of the network. As the bulkiness increased, ∼prestrain increased resulting in the network to become increasingly elastic as in the case of EUD_1-PEG_4 (hydrogel A). At smaller prestrain values (EUD_1-PEG_2), deformation seemed to be associated with the bending of Eudragit E100 fractions and the PEG 4000 filaments' angles remained close to their equilibrium values. As prestrain increased (EUD_1-PEG_4), the Eudragit E100 networks were progressively straightened and accompanied by changes in the angle between PEG 4000 complexed filaments. This stretching mechanism further resisted deformation by changing the extensional modulus (Figures 12 and 13). This corroborated with the experimental findings where hydrogel A had a continuous curve in which G′ was constantly >G″ indicative of a more elastic structure. Additionally, from Table IV it was clear that EUD_1-PEG_4 the angle energy was destabilized to a great extent (260.545 kcal mol^{-1}) and this bending caused an extensional stiffness of Eudragit E100 networks and PEG 4000 filaments played a defining role depending on the degree of prestrain. PEG 4000 filaments elevated the magnitude of G′ and reduced its gradient [Figure 4(a, b)], implying that the frequency dependence of G′ was reduced as networks incorporated more PEG 4000, as in the case of EUD_1-PEG_4. However, G″ increased slightly as the quantity of PEG 4000 increased, however, the gradient remained similar [Figure 4(a, b)]. Furthermore, Figure 12 demonstrated the highly stretched, stiffened, and strained network structure in hydrogel A compared to hydrogel B (Figure 12) rendering the latter to be an optimized structure with an appropriate rheological profile.

CONCLUSIONS

This study successfully implemented full characterization of the memblet system based on varying degrees of plasticizing. A greater plasticizing concentration (>30% w/v) did not drastically improve the physicomechanical and thermal properties of the memblet as was originally hypothesized. Rheologically, a 30% w/v of plasticizer concentration produced improved membrane flexibility that was essential for controlling gastric drug release. Thus, the plasticizing concentration at 30% w/v was encouraging as a minimal quantity of plasticizer is preferred for stable formulation. Optimization was based on the effect of other constituents of the memblet such as plasticizer and surfactant content. Accordingly, the characterization of the various plasticizing concentrations with optimal characterization parameters made it appropriate to propose that hydrogel B was more suited for memblet formation and gastric release of the model drug rifampicin. MM simulations corroborated the experimental findings. Drug release studies were crucial for justifying the function of the memblet system for application in gastric drug delivery.

REFERENCES

1. Deli, M. A. *Biochim. Biophys. Acta. Biomembr.* **2009**, *1788*, 892.
2. Lloyd, J. B. *Adv. Drug Deliv. Rev.* **2000**, *41*, 189.
3. Fan, Q.; Sirkar, K. K.; Michniak, B. *J. Membr. Sci.* **2008**, *321*, 240.
4. Branco, M. C.; Schneider, J. P. *Acta. Biomater.* **2009**, *5*, 817.
5. Nagahama, H.; Maeda, H.; Kashiki, T.; Jayakumar, R.; Furuike, T.; Tamura, H. *Carbohydr. Polym.* **2009**, *76*, 255.
6. Lee, K.; Shin, K-Y.; Yang, Y. S.; Shin, J-I.; Park, Y-C.; Seo, J-H.; Park, T. H.; Shin, C-S.; Jin, Y-S.; Kweon, D-H. *Enzyme Microb. Tech.* **2009**, *44*, 217.
7. Enescu, D.; Hamciuc, V.; Ardeleanu, R.; Cristea, M.; Loanid, A.; Harabagiu, V.; Simionescu, B. C. *Carbohydr. Polym.* **2009**, *76*, 268.
8. Nair, L. S.; Laurencin, C. T. *Adv Biochem. Eng. Biotechnol.* **2006**, *102*, 47.
9. Lee, K. Y.; Yuk, S. H. *Prog Polym. Sci.* **2007**, *32*, 669.
10. Rajagopal, K.; Schneider, J. P. *Curr. Opin. Struct. Biol.* **2004**, *14*, 480.
11. Branco, M. C.; Joel, P. *Acta Biomater.* **2009**, *5*, 817.
12. Lin, C-C.; Metters, A. T. *Adv. Drug. Deliv. Rev.* **2006**, *58*, 1379.
13. Ruel-Gariepy, E.; Leroux, J. C. *Eur. J. Pharm. Biopharm.* **2004**, *58*, 409.
14. Cabañas, M. V.; Peña, J.; Román, J.; Vallet-Regí, M. *Eur. J. Pharm. Sci.* **2009**, *37*, 249.
15. Wong, D. W. S.; Gastineau, F. A.; Gregorski, K. S.; Tillin, S. J.; Pavlath, A. E. *J. Agri. Food Chem.* **1992**, *40*, 540.
16. Francis, S. J. K.; Matthew, H. W. T. *Biomaterials* **2000**, *21*, 2589.
17. de Oliveira, H. P.; Albuquerque, J. J. F., Jr.; Nogueiras, C.; Rieumont, J. *Int. J. Pharm.* **2009**, *366*, 185.
18. Moustafine, R. I.; Kemenova V. A.; den Mooter, V. *Int. J. Pharm.* **2005**, *294*, 113.
19. Cui, F.; Wang, Y.; Wang, J.; Feng, L.; Ning, K. *Colloid Surf. A.* **2007**, *307*, 137.
20. Kohri, N.; Iwasa, K.; Kurihara, J.; Miyazaki, K.; Arita, T. *Int. J. Pharm.* **1989**, *49*, 213.
21. Moustafine, R. I.; Kemenova, V. A.; van den Mooter, G. *Int. J. Pharm.* **2005**, *294*, 113.
22. Goddeeris, C.; Willems, T.; Houthoofd, K.; Martens, J. A.; van den Mooter, G. *Eur. J. Pharm. Biopharm.* **2008**, *70*, 861.
23. Kabanova, T. V.; Zhdanova, E. R.; Moustafine, R. I. *J. Control. Release* **2006**, *16*, e33.
24. Ausar, S. F.; Bianco, I. D.; Castagna, L. F.; Alasino, R. V.; Beltramo, D. M. *J. Agri. Food Chem.* **2003**, *51*, 4417.
25. Tanner, R. I.; Qi, F.; Dai, S-C. *J Non-Newtonian Fluid Mech.* **2008**, *148*, 33.
26. Sozer, N. *Food hydrocolloid.* **2008**, *23*, 849.
27. Zhao, Q.; Sun, J.; Ling, Q.; Zhou, Q. *Langmuir* **2009**, *25*, 3249.
28. Peppas, N. A., Wood, K. M.; Blanchette, J. O. *Exp. Opin. Biol. Ther.* **2004**, *4*, 1.
29. Miyazaki, K.; Wyss, H. M.; Weitz, D. A.; Reichman, D. R. *Europhys. Lett.* **2006**, *75*, 915.
30. Hyun, K.; Wilhelm, M.; Klein, C. O.; Cho, K. S.; Nam, J. G., Ahn, K. H.; Lee, S. J.; Ewoldt, R. H.; McKinley, G. H. *Prog. Polym. Sci.* **2011**, *36*, 1697.
31. Mezger, T. G. In The Rheology Handbook: For Users of Rotational and Oscillatory Rheometers; Zorll, U., Ed.; Vincentz: Hannover (Germany), **2002**; p 26.
32. Lee, S. K.; Anema, S. G. *Food Chem* **2009**, *115*, 1373.
33. Uslu, I.; Keskin, S.; Gül, A.; Karabulut, T. C.; Aksu, M. L. *Hacettepe J. Biol. Chem.* **2010**, *38*, 19.
34. Feldstein, M. M.; Shandryuk, G. A.; Plate, N. A. *Polymer* **2001**, *42*, 971.
35. Gal, A.; Nussinovitch, A. *Int. J. Pharm.* **2009**, *370*, 103.
36. Yang, L.; Paulson, A. T. *Food Res. Int.* **2000**, *30*, 563.